Supramolecular Coordination Polymers: Viscosimetry and Voltammetry

J. van der Gucht,* N. A. M. Besseling, and H. P. van Leeuwen

Dutch Polymer Institute/Wageningen University, Laboratory of Physical Chemistry and Colloid Science, Dreijenplein 6, 6703 HB Wageningen, The Netherlands

Received: September 25, 2003; In Final Form: December 16, 2003

The formation of water-soluble coordination polymers was studied for a bifunctional monomer consisting of two terpyridin groups bridged by a poly(ethylene oxide) spacer. The complex formation between the terpyridin ligand groups and Cd^{2+} ions was demonstrated using UV/vis spectroscopy and potentiometric titration. Viscosimetry and voltammetry were used to study the formation of cadmium-based supramolecular coordination polymers as a function of the metal/monomer ratio and the total monomer concentration. An increase of the average degree of polymerization results in an increase of the viscosity and a decrease of the diffusion-limited voltammetric current. The results were interpreted using a theoretical model for the coordination polymerization into chains and rings. Very good, quantitative agreement was found between experiment and theory.

1. Introduction

Supramolecular polymers, chains of molecules connected by noncovalent bonds, have attracted considerable interest in recent years.[1−6] They have many properties in common with ordinary, covalent polymers, but also introduce new features. For example, the reversibility of the bonds between the monomers allows them to adapt their length distribution in response to environmental changes. If the association and dissociation of the bonds are rapid compared to the experimental time scale, the chain length distribution in these systems is determined by thermodynamic equilibrium.

A special class of supramolecular polymers is that of coordination polymers, in which the bonds between monomers are based on metal−ligand interactions (see Figure 1).[7−16] A number of coordination polymers have been synthesized, mostly based on kinetically inert complexes.[7−9] Exchange of ligands is extremely slow for these complexes, so that the chain length distribution is effectively frozen. Only a few *reversible* coordination polymers have been reported,[10,11] in which the bonds between monomers are formed by dynamic complexes.

In a recent paper,[16] reversible water-soluble coordination polymers were described, based on bifunctional monomers consisting of pyridine-2,6-dicarboxylic acid groups bridged by a short ethyleneoxide spacer. Viscosity measurements and ^1H NMR were used to follow the formation of polymers in solutions of these monomers with Zn^{2+} ions. The experimental results were interpreted using a theoretical model for the coordination polymerization into chains and rings.

In this paper, we consider supramolecular coordination polymers formed by bifunctional monomers with terpyridin ligand groups bridged by a poly(ethyleneoxide) spacer. The formation of supramolecular polymers with Cd^{2+} is studied using viscosity measurements and voltammetry, and the experimental results are compared quantitatively to the model of ref 16. A brief description of the model is given in section 2.1. In sections 2.2 and 2.3, we relate the distributions of chains and rings to the viscosity and the voltammetric limiting current.

* To whom correspondence should be addressed. E-mail: jasper.vandergucht@wur.nl.

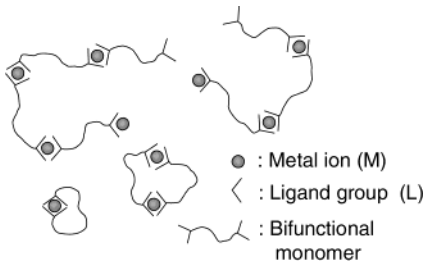

Figure 1. Schematic representation of a solution of coordination polymers with chains and rings.

Experimental details are presented in section 3, and the experimental results are discussed and compared to the model in section 4.

2. Theoretical Background

2.1. Coordination Polymers: Chains and Rings. The model developed in ref 16 for the chain/ring equilibrium in solutions of reversible coordination polymers is based on the theory of Jacobson and Stockmayer for polycondensation polymers.[17] In this section, we give a brief summary of the model.

We consider a solution of bifunctional ligands ("monomers") and metal ions (M), see Figure 1. Every monomer has two identical ligand groups L bridged by a spacer. The ligand groups can form two types of complexes with the metal ions: a 1:1 complex ML in which a metal ion is coordinated by one ligand group (and one or more solvent molecules) and a 1:2 complex ML_2 in which a metal ion is coordinated by two ligand groups. The ML_2 complexes form the bonds between the monomers, whereas the ML complexes and the free ligand groups L constitute the chain ends (see Figure 1). The strength of the two types of complexes is given by their stability constants:

$$K_1 = \frac{[ML]}{[M][L]} \tag{1}$$

$$K_2 = \frac{[ML_2]}{[ML][L]} \tag{2}$$

10.1021/jp036865r CCC: $27.50
Published on Web 02/03/2004

where [L], [M], [ML], and [ML_2] are the molar concentrations of free ligand groups, free metal, and ML and ML_2 complexes, respectively. We assume that the stability constants K_1 and K_2 do not depend on the degree of polymerization.

When metal ions and bifunctional monomers are mixed, two types of complexes can be formed (see Figure 1): chains and rings. We are interested in the distribution of monomers over chains and rings and in their length distributions. For the concentration $c(n, m)$ of chains of n monomers and m metal ions (with $|m - n| \leq 1$), the following equation was derived:[18]

$$c(n, m) = X_C C_{mon} A_{n-m} (pq)^{n-1} \tag{3}$$

Here X_C is the fraction of monomers incorporated in open chains, and C_{mon} is the total concentration of monomers. The factor p is the fraction of ligand groups in chains that are coordinated to a metal ion, and the factor q is the fraction of these coordinated ligand groups that is involved in an ML_2 complex. The probabilities p and q are determined by the stability constants K_1 and K_2 and by the monomer and metal concentrations. The factor A_{n-m} accounts for the probabilities of the two chain ends and depends on the type of ends of the chain (free ligand group L or ML complex), see ref 16.

For the concentration $r(n)$ of rings of n monomers (and n metal ions, as the number of monomers and metal ions are equal in a ring), the following equation was derived:[16,17]

$$r(n) = Bn^{-5/2}(pq)^n \ (n\nu \geq 1)$$
$$\text{with } B = \frac{10^{24}}{2N_{Av}b^3}\left(\frac{3}{2\pi\nu}\right)^{3/2} \tag{4}$$

where N_{Av} is Avogadro's number, b is the length of a statistical (Kuhn) segment expressed in nanometers, and ν is the number of Kuhn segments per monomer. The prefactor B has the dimension of moles per liter (so that $r(n)$ is expressed in moles per liter, too). It can be seen that rings of many monomers ($n \gg 1$) are very unlikely. As a result, the average length of the rings is much smaller than that of the chains. Furthermore, for very long spacers ($\nu \gg 1$) or very stiff spacers ($b \gg 1$), rings become less important.

Equation 4 was derived assuming that the chains satisfy Gaussian chain statistics. This is a reasonable assumption for chains and rings that are much longer than the Kuhn length ($n\nu \gg 1$). For monomers with a long spacer ($\nu \gg 1$), the Gaussian chain approximation is quite good even for the shortest chains and rings consisting of one monomer (if swelling of the chains due to excluded volume interactions is neglected).

The distributions of chains and rings depend on the total monomer concentration C_{mon}, on the metal-to-monomer ratio $y \equiv C_M/C_{mon}$, on the length ν and stiffness b of the monomers, and on the stability constants K_1 and K_2. As discussed in ref 16, for given values of these parameters, the probabilities p and q and the fraction of monomers in rings X_C can be calculated, giving the complete distributions $c(n, m)$ and $r(n)$. In ref 16, we presented theoretical predictions for the fractions of monomers in chains and rings and their average length. It was found that rings are most predominant at low monomer concentrations and at equal amounts of metal and monomers. Chains dominate at high monomer concentrations. The average length of the rings remains very small: most rings contain only one or two monomers (if $\nu > 1$). The average length of the chains, on the other hand, is much larger and increases with increasing monomer concentration. We compared the predictions of the model to viscosity and NMR measurements for a water-soluble Zn^{2+}-based coordination polymer. The experiments were in good qualitative agreement with the model. A more quantitative comparison was not made, however, because the monomers were too small ($\nu \approx 1$) for the Gaussian chain approximation to give quantitatively correct results. In this paper, we will present experimental results for coordination polymers consisting of monomers with a longer spacer ($\nu \gg 1$) for which a quantitative comparison is possible. To be able to do this, we need to link the model to experimentally accessible quantities such as the viscosity and the average diffusion coefficient measured with voltammetry. This will be done in the following sections.

2.2. Viscosity of Coordination Polymer Solutions. With the model described in the previous section, the distributions of chains and rings can be calculated for a solution of coordination polymers. If additional assumptions are made about the relation between the length and concentration of chains and rings and the viscosity, we can calculate the viscosity of the solution.

We consider only dilute solutions here, i.e., the polymers are not entangled. Following Duyndam and Odijk,[19] we assume that the zero-shear viscosity is determined by the equilibrium chain length distribution and is not affected by the reversible scission reactions of the bonds between the monomers. We furthermore neglect all interactions between different chains or rings. This will hold at low concentrations. The total viscosity of the solution is then simply a sum of the contributions of all chains and rings:

$$\eta_{sp} = M\sum_{n=1}^{\infty}(nc(n)[\eta]_n^C + nr(n)[\eta]_n^R) \tag{5}$$

Here $\eta_{sp} = (\eta - \eta_0)/\eta_0$ denotes the specific viscosity, with η and η_0 being the viscosity of the solution and that of the solvent, respectively. The first term in the sum is the contribution of the chains with $[\eta]_n^C$ being the intrinsic viscosity (in l/g) and $Mnc(n)$ being the weight concentration of chains of n monomers (with M the molecular weight of one monomer and $c(n) = \sum_m c(n, m)$ the molar concentration of chains of n monomers). Note that we include only the weight of the monomers and not that of the metal ions: we assume that the intrinsic viscosity of a chain depends only on the number of monomers (n) in the chain and not on the number of metal ions (m). This is reasonable because the monomers are much larger than the metal ions. The second term in eq 5 gives the contribution of the rings with $[\eta]_n^R$ the intrinsic viscosity of rings of n monomers and $Mnr(n)$ their weight concentration.

For the intrinsic viscosities of chains and rings, we use the well-known Mark−Houwink relations:

$$[\eta]_n^C = K_C n^{a_C} \quad \text{and} \quad [\eta]_n^R = K_R n^{a_R} \tag{6}$$

where K_C, K_R, a_C, and a_R are constants, depending on the structural details of the monomers. It has been shown theoretically that $a_C = a_R$.[20−22] Here, we use $a_C = a_R = 0.5$ which is the value obtained for chains and rings obeying Gaussian statistics (i.e., no excluded volume interactions). The intrinsic viscosity of a ring is smaller than that of a chain of the same length, because the structure of a ring is more compact. Hence, $K_R < K_C$. Theoretically, it has been shown that $K_R/K_C = 0.5$ for chains without intramolecular hydrodynamic interactions[20] and $K_R/K_C = 0.65$ for chains with intramolecular hydrodynamic interactions.[21,22] Here, we use the latter value (0.65), which seems to agree with most experimental findings.[23]

2.3. Voltammetry. 2.3.1. Voltammetry of Metal Ions. Voltammetry is a frequently used technique for the study of metal ions and their complexes.[24,25] The relevant experimental quantity is the limiting current i_L, which can be used to obtain information about the diffusion coefficient of the metal. For a stationary planar electrode, i_L is given by the Cottrell equation:[24−26]

$$i_L = \frac{zFAD_M^{1/2}C_M}{(\pi t)^{1/2}} \tag{7}$$

where z is the number of electrons involved in the electrode reaction, F is the Faraday constant, A is the surface area of the electrode, D_M is the diffusion coefficient, C_M is the bulk concentration of the metal ion, and t is the effective time of potential application. Equation 7 can also be used for spherical electrodes (e.g., a mercury drop) if the radius of curvature is much larger than the thickness of the diffusion layer (which is true for sufficiently small t).[25]

2.3.2. Voltammetry of Coordination Polymers. The presence of metal-binding ligands usually has a significant effect on the limiting current.[26−29] We use this effect to obtain information about the distribution of diffusion coefficients in a solution of coordination polymers. For coordination polymers, two types of complexes are important: ML complexes that constitute the chain ends (together with free ligand groups L) and ML_2 complexes that form the bonds between monomers. In general, the limiting current is determined by both the association/dissociation kinetics of these complexes and the diffusive transport toward the electrode.[30,31] The relative importance of these two processes is related to the lability of the complexes under the experimental conditions. This is conveniently expressed by a lability parameter ξ, which gives the ratio between the kinetic flux resulting from the dissociation of the complexes and the diffusive flux of complexes to the interface. For $\xi \gg 1$, the complexes are denoted as labile, whereas for $\xi \ll 1$, the complexes are called nonlabile. Under conditions of excess ligand, the lability parameter for an ML complex at the end of a particular chain is given by[32]

$$\xi_{ML} = k_{d,1}\left(\frac{D_M t}{k_{a,1}D_C[L]}\right)^{1/2} \tag{8}$$

where D_C is the diffusion coefficient of the chain and D_M is that of the free metal ion. The parameters $k_{d,1}$ and $k_{a,1}$ are the dissociation and association rate constants of an ML complex (these are related to the stability constant of an ML complex by $K_1 = k_{a,1}/k_{d,1}$), and [L] denotes the concentration of free (uncomplexed) ligand groups. We note that the diffusion coefficient D_C of a chain decreases with increasing chain length (see section 2.3.3), so that ξ_{ML} is larger for longer chains. For an ML_2 complex, the lability parameter can be expressed as[33]

$$\xi_{ML2} = \xi_M\frac{[ML]}{[ML_2]} \tag{9}$$

For excess ligand conditions, ML_2 is the dominant species (if $K_2 \gg 1$), so that $\xi_{ML_2} < \xi_{ML}$: ML_2 complexes are less labile with respect to dissociation into free metal than are ML complexes. For excess-metal conditions, eqs 8 and 9 are not applicable. The labilities of the complexes increase compared to the excess-ligand situation, but it is not known by how much.[34]

Labile Complexes (ξ_{ML2}, $\xi_{ML} \gg 1$). For labile complexes, the association/dissociation kinetics are so rapid that complexation equilibrium is maintained on the relevant scales in place and time. The limiting current is then determined by the coupled diffusion of free metal and the complexes. This proceeds with an overall mean diffusion coefficient $\bar{D}$, which takes into account the contribution of each form (chains and rings) weighted with its proportion, its diffusion coefficient, and the number of metal ions it contains. As a result of the net consumption of metal at the electrode, the concentration distributions for the different species in the diffusion layer are different from those in the bulk. This makes an exact calculation of the limiting current for this case very difficult.[35] For a large excess of ligand, the gradient in the ligand concentration is insignificant and it can be assumed that the relative proportions of the various species are constant throughout the diffusion layer.[27] For this case, the normalized limiting current is simply

$$\phi = \frac{i_L}{i_L^0} = \left(\frac{\bar{D}}{D_M}\right)^{1/2} \tag{10}$$

where i_L^0 is the limiting current of a solution containing the same concentration of metal, but no ligands, and where $\bar{D}$ is the mean diffusion coefficient:

$$\bar{D} = \frac{[M]D_M + \sum_{n,m}c(n,m)mD_{n,m}^C + \sum_n r(n)nD_n^R}{C_M} \tag{11}$$

Here [M], $c(n, m)$, and $r(n)$ denote the concentrations of free metal, chains, and rings in the bulk, $D_{n,m}^C$ is the diffusion coefficient of a chain of n monomers and m metal ions, and D_n^R is the diffusion coefficient of a ring of n monomers and metal ions. If there is no excess of ligand, eq 11 does not apply. For ligands that can only form one type of complex (ML), a numerical procedure was developed to relate the limiting current to the speciation for any metal-to-ligand ratio.[35] For coordination polymers, however, for which many different types of complexes can be formed, such a procedure is more involved, and outside the scope of this work.

Nonlabile Complexes (ξ_{ML2}, $\xi_{ML} \ll 1$). For $\xi \ll 1$, there is no significant dissociation of the complex during transport to the electrode. Every electroactive species has its own diffusion layer. The limiting current is the sum of the contributions of the free metal and the complexed metal. The former is proportional to $D_M^{1/2}[M]$ (see eq 7). This becomes very small for excess ligand conditions (when $[M] \approx 0$). The contribution of the complexed metal depends on whether the complexes are electroactive or not. If the complexes are not electroactive, they contribute to the current only via dissociation. This current is limited by the dissociation rate k_d of the complexes (and does not depend on time or on the diffusion coefficients of the complexes). For the trivial case that $k_d t \ll 1$ (i.e., inert complexes that do not dissociate on the experimental time scale t), the bound metal does not contribute to the current at all.

The situation becomes different if the complexes themselves are electroactive, i.e., if they can be reduced directly at the electrode.[27] For nonlabile electroactive complexes, there is no significant dissociation of the complex during the transport to the electrode, and the metal is only released in the course of the electron-transfer reaction at the electrode surface. The limiting current for this case is a sum of the separate contributions of the various complexes and is diffusion-limited because all of the separate contributions are diffusion limited. For a solution of coordination polymers, with chains and rings, this

gives the following normalized limiting current:

$$\phi = \frac{[\mathrm{M}]D_{\mathrm{M}}^{1/2} + \sum_{n,m} c(n,m)m(D_{n,m}^{\mathrm{C}})^{1/2} + \sum_{n} r(n)n(D_{n}^{\mathrm{R}})^{1/2}}{C_{\mathrm{M}}D_{\mathrm{M}}^{1/2}} \tag{12}$$

Here, the first term in the numerator is the contribution of the free metal, the second that of the chains, and the last one that of the rings. Note that the limiting current given by eq 12 is always smaller than that given by eqs 11 and 10.

We conclude that if the limiting current is diffusion-controlled, there are two possibilities. If $\xi \gg 1$, the complexes are fully labile, and the limiting current is given by eqs 11 and 10 (for excess ligand conditions). If ξ is on the order of unity or smaller and the limiting current is still diffusion controlled (while being larger than the limiting current for the metal alone), then the complexes *must* be electroactive. The limiting current is then given by eq 12 (for $\xi \ll 1$).

2.3.3. Diffusion Coefficients. Equations 11 and 10 or eq 12 relate the limiting current to the distribution of diffusion coefficients of chains and rings. The diffusion coefficient of a chain or ring is related to its size by the Stokes−Einstein relation:

$$D_i = \frac{kT}{6\pi\eta R_i} \tag{13}$$

where η is the viscosity of the medium, and R_i is the hydrodynamic radius of a species *i*. This radius is determined by the length of the chain or ring. We assume here that chains with the same number of monomers have the same radius, irrespective of the number of metal ions (i.e., it does not matter whether the termination is by free ligand groups or by ML complexes). For Gaussian chains and rings, the hydrodynamic radius is proportional to the square root of the length. Hence, we find the following expressions for the ratio between the diffusion coefficient of a chain or ring and that of a free metal ion in a solution containing no monomers (with viscosity η_0):

$$\frac{D_n^{\mathrm{C}}}{D_{\mathrm{M}}} = \frac{\alpha_{\mathrm{C}}}{n^{1/2}}\frac{\eta_0}{\eta} \quad \text{and} \quad \frac{D_n^{\mathrm{R}}}{D_{\mathrm{M}}} = \frac{\alpha_{\mathrm{R}}}{n^{1/2}}\frac{\eta_0}{\eta} \tag{14}$$

From the combination of eq 14 with eq 13, it follows that α_{C} and α_{R} are equal to the ratio between the hydrodynamic radius of a metal ion and that of an open chain or closed ring monomer, respectively. They depend on the length of a monomer ν and the Kuhn length *b*. Because a ring is more compact than a chain of the same size, it feels a smaller friction. Hence, $\alpha_{\mathrm{R}} > \alpha_{\mathrm{C}}$. For Gaussian chains without excluded volume interactions, Bloomfield and Zimm have predicted $\alpha_{\mathrm{R}}/\alpha_{\mathrm{C}} = 1.18$,[21] which has been confirmed experimentally.[23] Here, we will use the same value.

3. Experimental Section

Materials. The bifunctional monomers (bisterpyridine terminated poly(ethylene oxide), denoted as T_2EO, see Figure 2) were kindly provided by Dr. Schmatloch and Prof. Schubert from Technical University Eindhoven (see refs 13−15 for details about the synthesis). The number average molar mass was estimated using MALDI-TOF-mass spectrometry: $M = 9570$ g/mol.[36] This corresponds to a number average of 207 ethylene oxide units per spacer. The complexation of the ligands with several transition metal ions was demonstrated using UV/vis spectroscopy.[13,14] Viscosity measurements were used to study the formation of supramolecular polymers in methanol and water.[15] Here, we prepared aqueous solutions of the bifunctional monomers in a 0.01 M MOPS (morpholino propane sulfonic acid) buffer (pH 6.0) at 1.0 M KNO_3 (unless otherwise specified). This gave clear, colorless, low-viscosity solutions. The metal salt was $Cd(NO_3)_2$. All measurements were done at 25 °C. Unfunctionalized poly(ethylene oxide) of molar mass 8000 g/mol was obtained from Sigma.

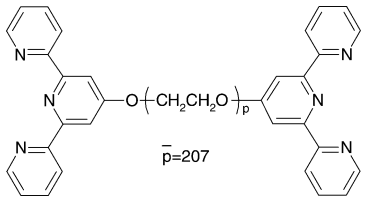

Figure 2. Schematic representation of bifunctional ligand T_2EO, consisting of two terpyridin groups (ligands) bridged by a PEO spacer.

Complexation Behavior. The complexation of the molecules with Cd^{2+} was investigated using UV/vis spectroscopy and potentiometric titration. UV/vis measurements were done by adding a concentrated $Cd(NO_3)_2$ solution to the ligand solution and recording changes in the spectra. The absorption coefficient was calculated as $\epsilon = A/(cl)$ with *A* being the absorbance, *c* being the monomer concentration (in mol/m^3), and *l* being the path length (in m). Because of UV absorption of the electrolyte, these measurements were done at 0.01 M KNO_3 instead of 1 M.

Potentiometric titrations (at 1.0 M KNO_3) were done by adding a concentrated $Cd(NO_3)_2$ solution to the ligand solution and measuring the potential difference between a Cd-solid-state electrode and a reference electrode (Ag/AgCl/saturated KCl). The Cd electrode was calibrated using Cd^{2+} solutions of known concentration without ligand at the same electrolyte and buffer concentration. Calibration plots of the potential *E* versus log[Cd^{2+}] were linear for the concentration range used (total cadmium concentration between 10^{-4} and 2×10^{-3} M), with a slope of 26.5 mV.

Viscosity Measurements. Viscosity measurements were performed in a PVS1 LAUDA capillary viscosimeter. A concentrated $Cd(NO_3)_2$ solution was added stepwise to a solution containing bifunctional ligands (in 0.01 M MOPS buffer of pH 6.0 and at 1.0 M KNO_3). The Hagenbach-corrected run-through time *t* was measured and compared to that of pure buffer without ligands t_0. The specific viscosity was calculated as

$$\eta_{\mathrm{sp}} = \frac{\eta - \eta_0}{\eta_0} = \frac{t - t_0}{t_0} \tag{15}$$

where η and η_0 denote the viscosity of the solution and of pure buffer, respectively.

Voltammetry. Measurements were performed using the AUTOLAB system (Ecochemie) in conjunction with a Metrohm 663 VA stand with multimode mercury electrode. The auxiliary electrode was glassy carbon, and the reference electrode was Ag/AgCl/saturated KCl. Dissolved oxygen was removed by bubbling argon through the solution prior to each measurement. We used both normal pulse (NP) and reverse pulse (RP) modes with pulse times varying between 25 and 150 ms. For every pulse, a new mercury drop was used, and the time between successive drops was 1 s. For NP, the potential between the pulses was maintained at −0.3 V (well before the reduction wave of Cd^{2+}). For RP, the potential between the pulses was kept at −1.2 V (in the limiting current regime). The scan rate was 10 mV/s.

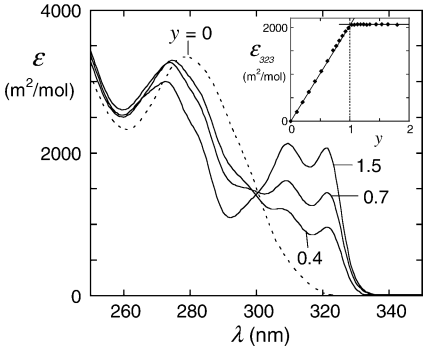

Figure 3. UV/vis spectra of monomers T_2EO for various metal/monomer ratios y, $[T_2EO] = 2.0 \times 10^{-5}$ M. Inset: Absorption coefficient at 323 nm as a function of y.

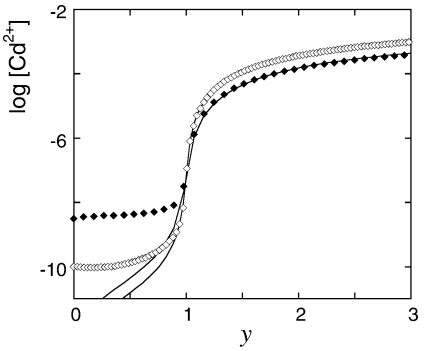

Figure 4. Titration of T_2EO with Cd^{2+}: concentration of free cadmium as a function of $y = C_M/C_{mon}$ for two monomer concentrations: 0.74 mM (◆) and 2.1 mM (◇). Full curves are fits to the data with $K_1 = 1.3 \times 10^7$ and $K_2 = 1.6 \times 10^6$.

We used a high electrolyte concentration (1 M KNO_3) in order to minimize migration currents and a 0.01 M MOPS buffer of pH 6.0. A concentrated solution of $Cd(NO_3)_2$ was added in small steps to 5 mL of monomer solution, or vice versa. After every addition, voltammograms were recorded (NP and RP, using several pulse times). These voltammograms were compared to those of solutions containing only metal at the same concentration, and the normalized limiting current $\phi = i_L/i_L^0$ was calculated. In all cases, NP and RP voltammograms gave the same results for ϕ, indicating that limiting currents are not obscured by reactant adsorption (another indication for this is that we never observed maxima in the NP waves).[37]

4. Results and Discussion

4.1. Complexation Behavior. In Figure 3, we show the UV/vis spectrum of a solution of bifunctional ligands T_2EO with different amounts of added metal. Clearly, the absorption bands of the terpyridin groups are shifted after addition of Cd^{2+} as a result of complex formation. The inset shows the height of the peak at 323 nm as a function of the ratio $y \equiv C_M/C_{mon}$. For $y < 1$, the absorbance at 323 nm increases linearly with increasing y, due to an increasing amount of complexed ligand groups. For $y > 1$, the absorption remains constant. This indicates that the metal ions and monomers bind in a 1:1 ratio, corresponding to ML_2 complexes. This is the right stoichiometry for coordination polymers to be formed.

In Figure 4, potentiometric titration curves are shown. The concentration of free metal (determined from the potential of the Cd electrode using the calibration data) is shown as a function of the ratio between metal and monomers for two monomer concentrations. At low cadmium concentrations, nearly all of the metal is bound to ligand groups so that the free metal concentration is very low. When the equivalence point ($y = 1$) is reached, the concentration of free cadmium increases strongly, again indicating the formation of ML_2 complexes. The data of Figure 4 can be used to obtain estimates for the stability constants of the complexes. For $y > 1$, the data can be fitted using two stability constants: one for the ML complex (K_1, eq 1) and one for the ML_2 complex (K_2, eq 2). These fits are shown in Figure 4. At low metal concentrations, the data cannot be fitted adequately. Apparently, the Cd-solid-state electrode cannot be used for the present ligands in this regime. Due to the poor fit at low metal concentrations, the values obtained for the stability constants are not very accurate. Nevertheless, we get a rough estimate:

$$\log K_1 = 7.1 \pm 0.4 \text{ and } \frac{K_1}{K_2} = 8 \pm 3$$

In ref 16 it was shown that the precise values of the stability constants are not very important for the distribution of complexes over chains and rings (as long as they are large enough). Even when the stability constants were changed by a factor of 10, the results were only slightly different. Therefore, we expect to get a rather good description of the properties of our system using the values for K_1 and K_2 obtained from the titrations.

To check that Cd^{2+} does not bind to the PEO spacer of the monomers, we performed a similar titration with unfunctionalized PEO, molar mass 8000 g/mol. No effect of PEO on the concentration of free Cd^{2+} was found, showing that Cd^{2+} binding to PEO is negligible under the experimental conditions used.

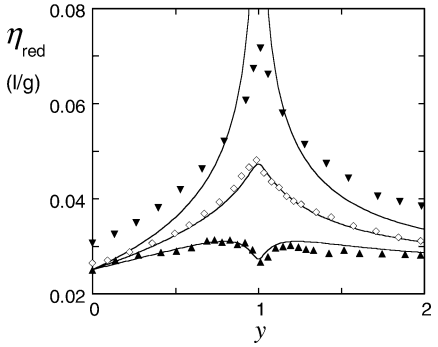

Figure 5. Reduced viscosity of a solution of T_2EO as a function of the cadmium/monomer ratio y for three different monomer concentrations: 0.50 mM (▲), 0.83 mM (◇), and 1.75 mM (▼). Full curves are fits through the data according to eq 5 with $K_C = 0.025$ g/L and $B = 3.6 \times 10^{-4}$ M.

4.2. Viscosity Measurements. In Figure 5, the reduced viscosity ($\eta_{red} = \eta_{sp}/(MC_{mon})$) of T_2EO is shown as a function of the molar ratio y for three concentrations of monomers. In the experiments, a concentrated solution of $Cd(NO_3)_2$ was added stepwise to the solution of monomers. After each addition, the solution was mixed for a few minutes and the viscosity was measured. We could not observe any time dependence, indicating that equilibrium is reached within a few minutes.

For the two highest concentrations, the viscosity increases with increasing amount of metal until a ratio of unity is reached. This is caused by an increase of the average length of the polymers as the number of free L-groups, which constitute chain ends, decreases. For $y > 1$, the viscosity decreases again. This decrease is a result of the formation of more and more ML complexes which also constitute chain ends, and thus decrease the average length. The conversion of ML_2 complexes into ML complexes for $y > 1$ indicates that the system is reversible, at

least on the time scale of several minutes. For the lower monomer concentration (0.5 mM), a different curve is obtained. At a metal/monomer ratio of unity, the viscosity exhibits a minimum, rather than a maximum. As explained in detail in a recent paper,[16] such a dip can be attributed to the formation of rings. It was shown that rings are most predominant at low monomer concentrations and at $y = 1$. Because rings are smaller and more compact than chains (see section 2.1), their enhancement of the viscosity is smaller.

We will now make a quantitative comparison between the experimental results and the model described in sections 2.1 and 2.2. The model contains four parameters: the stability constants K_1 and K_2, the Mark−Houwink constant for chains K_C, and the parameter B which depends on the length and stiffness of the spacer. Furthermore, we use $K_R/K_C = 0.65$ and $a_C = a_R = 0.5$ (see section 2.2). For the stability constants K_1 and K_2, we use the values obtained from the potentiometric titrations (section 4.1). The value of K_C can be obtained independently from the intercept with the viscosity axis in Figure 5. At this point, there are only monomers and no metal ions. It can be seen in Figure 5 that for the two lowest monomer concentrations the intercept with the vertical axis (giving the reduced viscosity of a solution of monomers without metal) is nearly the same, indicating that interactions between monomers are not very important for these concentrations. For the highest concentration, however, the intercept with the vertical axis is higher than for the other two concentrations. Hence, interactions cannot be neglected at this concentration. Since our model assumes noninteracting polymers, we cannot expect very good agreement between theory and experiment for this concentration. For the lowest concentrations, the viscosity at $y = 0$ is given by: $\eta_{red} \approx [\eta]_1^C$, where $[\eta]_1^C$ is the intrinsic viscosity of pure monomers (see eq 5 with $c(1, 0) = C_{mon}$ and $c(n, m) = r(n) = 0$ for $m > 0$). Using eq 6 (with $n = 1$), we then find $K_C \approx 0.025$ l/g.

The only remaining fit parameter is B. The full curves in Figure 5 show the resulting fits through the data points. All three curves are obtained with $B = 3.6 \times 10^{-4}$ M. We see that, for the two lowest concentrations, the experimental data are very well fitted by the model. As expected, for the highest concentration, the fit is not very good, because interactions between polymers cannot be neglected at this concentration. From the intercept with the vertical axis, we see that $\eta_{red} > [\eta]_1^C$ for this concentration, which indicates that the second virial coefficient for the monomers is positive. One would expect that this effect would only become larger as the chain length increases, but in Figure 5 we see that the experimental data points and the fit cross each other, so that the measured viscosity is lower than the calculated one for y around unity. A possible explanation for this could be that the solution at this concentration is shear thinning (for example, because the chains can break under shear), and that the measured viscosities at the highest concentration do not correspond to the zero-shear viscosity. In principle, this hypothesis could be tested by measuring the viscosity at different shear rates using a rheometer (we could not do this because of the limited amount of available material).

The value for B obtained from the fits can be used to estimate the Kuhn length b of the monomers using eq 4 and $\nu b = L$, where L is the contour length of a monomer. The average number of ethylene oxide units per monomer is 207 (see section 3), and the length of one ethylene oxide unit is about 0.36 nm. This gives $L \approx 75$ nm. Equation 4 then gives a value for the Kuhn length b of 1.1 nm (and $\nu = 67$). This is somewhat larger than values reported for poly(ethylene oxide) in the literature

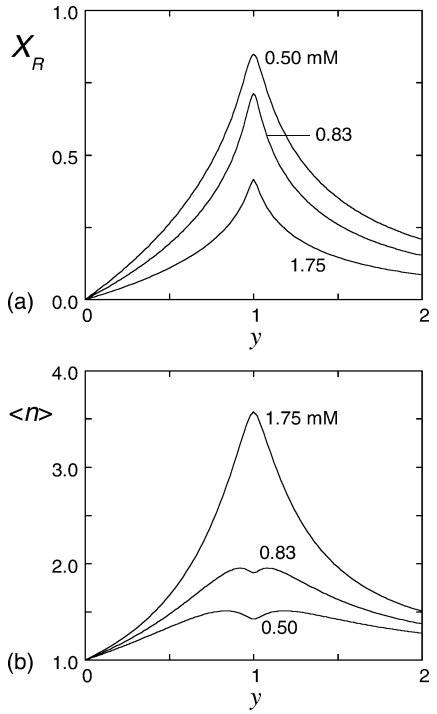

Figure 6. (a) Calculated fraction of monomers in rings X_R as a function of the metal/monomer ratio y for the same three concentrations as in Figure 5. (b) Average degree of polymerization $\langle n \rangle$ as a function of y for same concentrations.

($b \approx 0.75-0.8$ nm).[38,39] This difference is probably due to the approximations made in the model, in particular the neglect of excluded volume interactions between segments, that would lead to swelling of the chains in a good solvent.

Figure 6a shows the calculated fraction of rings as a function of the molar ratio metal/monomers for the same monomer concentrations as in Figure 5 (and for $B = 3.6 \times 10^{-4}$ M as used in the fits in Figure 5). This figure shows that rings are indeed most predominant at low concentrations and at a molar ratio of unity. The calculated number average degree of association $\langle n \rangle$ is shown in Figure 6b as a function of the molar ratio. It can be seen that the average length has a minimum at a molar ratio of unity for low monomer concentrations, as a result of the large number of small (predominantly monomeric) rings at this point. We note that the average degree of polymerization remains very low for the concentrations used. This is a result of the large fraction of small rings.

To be sure that the observed changes in the viscosity can be attributed to the formation of polymers as a result of complex formation between cadmium and the terpyridin groups and not by the PEO spacer, we also measured the viscosity of a solution of unfunctionalized PEO with varying amount of cadmium. No changes in the viscosity could be measured upon addition of metal. This indicates that there is no significant aggregation of the PEO-spacer as a result of complex formation with Cd^{2+} ions.

4.3. Voltammetry. In Figure 7a, normalized NP voltammograms are shown for solutions containing monomers and Cd^{2+} at several ratios. Figure 7b shows RP voltammograms for the same solutions. For Cd^{2+} solutions without monomers ($y = \infty$), the wave has a regular shape, typical for a reversible electrode reaction. The half-wave potential is at −0.55 V versus Ag/AgCl/saturated KCl. When monomers are added, the reduction wave shifts to more negative potentials and the limiting current decreases. The NP wave becomes broader, and in the RP voltammogram, we see that the reduction and oxidation waves

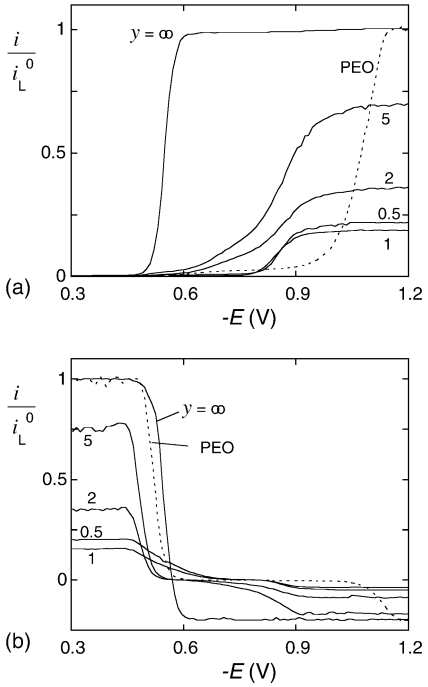

Figure 7. Normalized NP (a) and RP (b) waves for solutions of T_2EO (1.13 mM) with added Cd^{2+} at various ratios y. Dashed lines are voltammograms for Cd^{2+} with 10 g/L unfunctionalized PEO of molar mass 8000 g/mol.

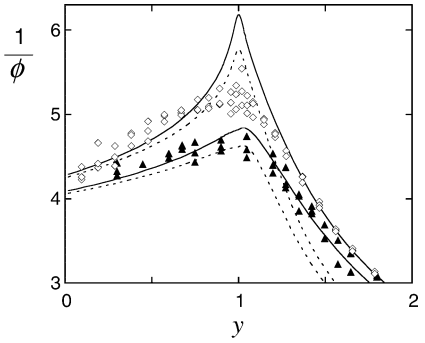

Figure 8. Reciprocal normalized current $1/\phi = i_L^0/i_L$ for T_2EO solutions as a function of $y = C_M/C_{mon}$ for monomer concentrations of 0.83 mM (▲) and 1.13 mM (◇). Full curves: fits to eq 12 (nonlabile electro-active complexes), dashed curves: fits to eq 10 (fully labile complexes). Fit parameters: $B = 3.6 \times 10^{-4}$ M and $K_C = 0.024$ g/L (as obtained from Figure 5), and $\alpha_C = 0.086$.

are separated by some 0.2−0.4 V. These phenomena are indicative for less reversible electrode processes, i.e., limited rates of electron transfer in the region before reaching the limiting current.[24]

To check whether the effect of the monomers on the voltammograms is due to complex formation with the terpyridin groups, and not to the PEO-spacer, we also recorded voltammograms for Cd^{2+} in the presence of unfunctionalized PEO (molar mass 8000, 10 g/L). These are also shown in Figure 7, parts a and b (the dashed curves). It can be seen that PEO has quite a large effect on the shape of the voltammogram: like for T_2EO, the reduction wave is shifted toward more negative potentials, and the oxidation and reduction waves in RP are separated. This suggests that the changes in the shape of the voltammograms upon addition of T_2EO are caused by the PEO spacer rather than by the complexation with the terpyridin groups. A possible explanation for the effect of PEO on the voltammograms is that the polymer chains adsorb at the surface of the mercury electrode in the potential range between −0.6 and −1 V and thereby hinder the electrode processes. It can be seen that the potential range where this hindrance occurs is smaller for the bifunctional monomers than for unfunctionalized PEO. Possible reasons for this are the difference in molar mass and the effect of the terpyridin groups that may modify the adsorption behavior of PEO.

We will not discuss the shape of the voltammograms in more detail here and focus only on the limiting currents. Whereas the shape of the cadmium wave changes significantly after addition of PEO, the limiting current remains the same. Hence, the diffusion coefficients of the metal species are not affected by PEO. This indicates that complexation of Cd^{2+} with the PEO backbone is negligible and is in agreement with our observations in sections 4.1 and 4.2. We may therefore conclude that the variations in the limiting currents observed for the bifunctional monomers are caused by complex formation with the terpyridin groups.

To check whether the limiting currents are diffusion controlled, we varied the pulse time and plotted i_L versus $t^{-1/2}$ (a so-called Cottrell plot). In all cases, we obtained linear plots with a small intercept with the vertical axis (which has been shown to be due to the spherical geometry[25]). Therefore, we conclude that the limiting currents are indeed diffusion controlled within the used time range (see also eq 7). Moreover, values of $\phi = i_L/i_L^0$ were the same for NP and RP, indicating that the limiting currents are not influenced by adsorption phenomena.[40]

The reciprocal normalized limiting currents $\phi^{-1} = i_L^0/i_L$ are plotted in Figure 8 as a function of the molar ratio y for two different monomer concentrations. Clearly, the limiting currents are smaller in the presence of monomers than without monomers. This is a result of the formation of complexes with diffusion coefficients that are smaller than that of free cadmium. The data in Figure 8 are rather similar to the viscosity plots shown in Figure 5. The normalized current first decreases (and ϕ^{-1} increases) with increasing amount of added metal until a ratio of unity is reached. This is a result of the increase of the average length (see Figure 6b), which causes a decrease of the average diffusion coefficient (see eq 14). This effect is enhanced by an increase of the viscosity, which also leads to a decrease of D. For $y > 1$, ϕ^{-1} decreases again. This is the result of the conversion of ML_2 complexes into ML complexes, which form extra chain ends. This leads to a decrease of $\langle n \rangle$ and η. At $y = 1$, ϕ^{-1} passes through a maximum, which becomes higher as the concentration increases. In the following, we will discuss the results more quantitatively, using the model described in sections 2.1 and 2.3.

All of the measured limiting currents in Figure 8 are diffusion controlled ($i_L \sim t^{-1/2}$). As discussed in section 2.3.2, this implies that the complexes are either fully labile or that they are electroactive and can be reduced directly at the electrode. An a priori estimate of the lability parameters ξ_{ML} and ξ_{ML_2} (eqs 8 and 9) can be obtained starting from the stability constants of the complexes. It may be expected that the association rate of the complexes is determined by the dehydration step of the metal ion (Eigen mechanism[41]). For Cd^{2+} this would give a rate constant $k_{a,1}$ of the order of 10^8 M^{-1} s^{-1}.[42] With $K_1 \approx 10^7$ M^{-1}, this gives $k_d \approx 10$ s^{-1}. If we furthermore assume that the ratio between the diffusion coefficients D_M/D_C is on the order of 10 (which is about the value of $1/\alpha_C$, see below), we obtain for a pulse time of 0.1 s $\xi_{ML} \approx 10^{-3}$ $[L]^{-1/2}$ and (with $K_2 = 10^6$ M^{-1}) $\xi_{ML_2} \approx 10^{-9}$ $[L]^{-3/2}$. For excess ligand conditions, [L] is on the order of 10^{-3} M, so that the ML complexes would be

partially labile and the ML_2 complexes (the dominant species in this regime) would be nonlabile. The diffusion-limited limiting current thus suggests that the complexes must be electroactive. Hence, we expect that eq 12 applies in this regime. For excess metal conditions, eqs 8 and 9 are not applicable, and it is uncertain whether the complexes are labile or not. The complexes are more labile than for the excess-ligand situation, but it cannot be estimated by how much.[34]

For fitting the data in Figure 8, we use the same values for the stability constants K_1 and K_2 and for the parameter B as for fitting the viscosity data in Figure 5. The diffusion coefficients of chains and rings depend on the viscosity of the solution and on the parameters α_C and α_R (eq 14). The viscosity can be calculated as described in section 2.2. We use $K_C = 0.025$ l/g, i.e., the value obtained from the fits in Figure 5. Furthermore, we use $\alpha_R/\alpha_C = 1.18$ (see section 2.3). This leaves one additional fit parameter, α_C.

All fits have been obtained with $\alpha_C = 0.086$. As explained in section 2.3.3, α_C is equal to the ratio between the hydrodynamic radius of a cadmium ion and that of a monomer. For free cadmium, a diffusion coefficient of 7.2×10^{-10} m^2/s has been reported (in 0.1 M KNO_3 at 298 K),[43] which corresponds to a hydrodynamic radius for Cd^{2+} of 0.30 nm. This gives a value of 3.5 nm for the hydrodynamic radius of a monomer, which is very close to the radius of gyration calculated using $b = 1.1$ nm and $\nu = 67$ (as obtained from the parameter B, see section 2.2): $R_g = b(\nu/6)^{1/2} \approx 3.7$ nm.

The full curves in Figure 8 are fits through the data points according to eq 12, i.e., assuming nonlabile electroactive complexes. The dashed curves are fits according to eqs 10 and 11, i.e., for fully labile complexes. As noted above, the estimated values of the lability parameters ξ_{ML} and ξ_{ML_2} suggest that the complexes are nonlabile for $y < 1$ (excess ligand) and electroactive. Indeed, we see that the fits to eq 12 (the full curves) describe the data rather well. The difference between the two fits for $y < 1$ is rather small, however, so that the data in Figure 8 cannot provide a decisive answer to the question whether the complexes are labile or not in this regime. For $y > 1$, the lability eqs 8 and 9 are not applicable. It can be seen in Figure 8 that eq 12 (full curves) works much better in this regime than eqs 10 and 11 (dashed curves). This does not necessarily mean that the complexes are nonlabile for $y > 1$, however. As discussed in section 2.3.2, eq 11 (for the labile case) is expected to fail for $y > 1$, because it neglects that the distributions of chains and rings in the diffusion layer are different from those in the bulk.

The agreement between the experimental data in Figure 8 and the fits according to eq 12 (nonlabile electroactive complexes) is rather good, especially for the lowest concentration. For $C_{mon} = 1.13$ mM, the model overestimates the height of the maximum, i.e., the model gives too low values for the limiting current in this regime. One possible explanation for the underestimation of the limiting current is that interactions between polymers cannot be neglected at high concentrations. This was also observed in the viscosity measurements (Figure 5) for the highest concentration of $C_{mon} = 1.75$ mM. Another explanation could be that the assumption of nonlabile complexes is not valid when $y \approx 1$. As can be seen from eqs 8 and 9, the lability of the complexes increases as [L] decreases, i.e., for increasing y. Indeed, we see in Figure 8 that the dashed curves (the labile case) are closer to the experimental data points than the full curves (the nonlabile case) when $y \approx 1$. A third reason for the difference between theory and experiment could be the inhomogeneity of the medium. In eq 14, we have assumed that the diffusing chains and rings experience a friction which is governed by the macroscopic viscosity. On the scale of a monomer, however, the medium is not homogeneous. The chains may therefore experience a friction which is smaller than that according to the macroscopic viscosity η (and more close to the solvent viscosity η_0).[44,45] This would result in a larger diffusion coefficient and, as a result, a larger limiting current. This effect is most important at high monomer concentrations, because the effect of the viscosity is largest there.

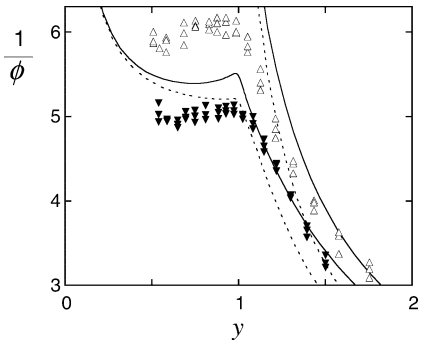

Figure 9. Reciprocal normalized current $1/\phi = i_L^0/i_L$ for cadmium/monomer solutions as a function of $y = C_M/C_{mon}$ for cadmium concentrations of 0.99 mM (▼) and 1.92 mM (△). Full curves are calculated with eq 12 (nonlabile electro-active complexes), and dashed curves with eq 10 (fully labile complexes), using the same parameters as in Figure 8.

We could also try to fit the data using the solvent viscosity η_0 rather than the solution viscosity η in eq 14. For the lowest concentration ($C_{mon} = 0.83$ mM) this hardly affects the results. The effect of the viscosity increase on the diffusion coefficient is much smaller in this case than the effect of the increase in average length. For $C_{mon} = 1.13$ mM, however, the viscosity does have a large effect on the fits. Fitting the data using η_0 instead of η would lead to an overestimation of the limiting current (and an underestimation of ϕ^{-1}). Hence, the real effective friction that the polymers experience lies probably between η_0 and η.

The data in Figure 8 were obtained by titrating a concentrated cadmium solution to a solution of monomers. We have also carried out the converse experiment, i.e., a titration of a cadmium solution with a concentrated monomer solution. The normalized limiting currents for these experiments are shown in Figure 9 for two cadmium concentrations. The predictions of the model, with the same values for the various parameters as used for fitting the data in Figure 8, are also shown in this figure for both limiting cases. It can be seen that the maximum in $1/\phi$ is less pronounced than in Figure 8. This can be understood by considering that variation of the molar ratio y has *two* effects in this case. First, as in Figure 8, the average size of the polymers passes through a maximum as a function of y (see Figure 6). At the same time, however, the monomer concentration increases monotonically with decreasing y (since C_M is fixed). This second effect results in an increase of the viscosity with decreasing y. Hence, for $y < 1$, the individual polymers become smaller with decreasing y (i.e., increasing amount of added monomers), but they have to diffuse through a medium with a higher viscosity. We also see in Figure 9 that the agreement between the experimental data and the calculated curves is not as good as in Figure 8, especially for $y < 1$, where the monomer concentration is rather high. Again, this is probably due to the interactions between chains that cannot be neglected in this regime or to the difference between the macroscopic viscosity and the local viscosity experienced by the polymers.

5. Concluding Remarks

We have studied the formation of coordination polymers based on complex formation between terpyridin ligand groups and Cd^{2+} ions in aqueous solution. The complex formation was demonstrated using UV/vis spectroscopy, and the stability constants were estimated from potentiometric titration data. Viscosimetry and voltammetry were used to study the formation of supramolecular polymers. The measurements were compared to a theoretical model for the polymerization of coordination polymers into chains and rings. At relatively low concentrations, both the viscosity of the solutions and the voltammetric limiting current were in very good agreement with the model calculations. This provides strong support in favor of the proposed model. We also tried to fit the data using a model which neglects the formation of rings, but this gave much worse agreement. At higher concentrations, the agreement between experiment and model is not very good, probably because interactions between different polymers are completely neglected in the model.

As noted in the Introduction, an important difference between supramolecular polymers and covalent polymers is their dynamic behavior. The dynamics of supramolecular polymers are governed by the rate constants of association and dissociation. Based on the measured stability constants, we estimated that $k_{a,1} \simeq 10^8\ M^{-1}s^{-1}$ and $k_{d,1} \simeq 10\ s^{-1}$. These values suggest that the polymers may be considered as reversible on the time scale of several seconds to minutes and that thermodynamic equilibrium should be reached on this time scale. This is in agreement with the fact that we never observed any time dependence in our measurements (which were typically carried out after mixing for a few minutes).

In principle, voltammetry can also provide information about the kinetics of the complexes, because labile and nonlabile complexes usually give rise to a very different limiting current. However, the data for the present system strongly suggest that the complexes are electroactive, i.e., that they can be reduced directly at the electrode. For electroactive complexes, the difference between a labile and a nonlabile response is much smaller. Our experimental data are not sufficiently accurate to distinguish between these two cases.

Acknowledgment. We are greatly indebted to Dr. Schmatloch and Prof. Schubert from Technical University Eindhoven for providing the bifunctional monomers.

References and Notes

(1) Lehn, J.-M. *Supramolecular Chemistry, Concepts and Perspectives*; VCH: Weinheim, Germany, 1995.
(2) Ciferri, A. *Supramolecular polymers*; Marcel Dekker: New York, 2000.
(3) Sijbesma, R. P.; Beijer, F. H.; Brunsveld, L.; Folmer, B. J. B.; Hirschberg, J. H. K. K.; Lange, R. F. M.; Lowe, J. K. L.; Meijer, E. W. *Science* **1997**, *278*, 1601.
(4) Boileau, S.; Bouteiler, L.; Lauprêtre, F.; Lortie, F. *New J. Chem.* **2000**, *24*, 845.
(5) Fogleman, E. A.; Yount, W. C.; Xu, J.; Craig, S. L. *Angew. Chem., Int. Ed.* **2002**, *41*, 4026.
(6) Zimmerman, N.; Moore, J. S.; Zimmerman, S. C. *Chem. Ind.* **1998**, 604.
(7) Chen, H. C.; Cronin, J. A.; Archer, R. D. *Macromolecules* **1994**, *27*, 2174.
(8) Kelch, S.; Rehahn, M. *Macromolecules* **1997**, *30*, 6185.
(9) Bernhard, S.; Takada, K.; Deaz, D.; Abruna, H. D.; Murner, H. *J. Am. Chem. Soc.* **2001**, *123*, 10265.
(10) Velten, U.; Rehahn, M. *Chem. Commun.* **1996**, 2639.
(11) Velten, U.; Lahn, B.; Rehahn, M. *Macromol. Chem. Phys.* **1997**, *198*, 2789.
(12) Schutte, M.; Kurth, D. G.; Linford, M. R.; Colfen, H.; Mohwald, H. *Angew. Chem., Int. Ed.* **1998**, *37*, 2891.
(13) Schubert, U. S.; Eschbaumer, C. *Angew. Chem., Int. Ed.* **2002**, *41*, 2892.
(14) Schubert, U. S.; Hien, O.; Eschbaumer, C. *Macromol. Rapid Commun.* **2000**, *21*, 1156.
(15) Schubert, U. S.; Eschbaumer, C. *Polym. Prepr.* **2000**, *42*, 395.
(16) Vermonden, T.; Van der Gucht, J.; De Waard, P.; Marcelis, A. T. M.; Besseling, N. A. M.; Sudholter, E. J. R.; Fleer, G. J.; Cohen Stuart, M. A. *Macromolecules* **2003**, *36*, 7035.
(17) Jacobson, H.; Stockmayer, W. H. *J. Chem. Phys.* **1950**, *18*, 1600.
(18) Flory, P. J. *Principles of Polymer Chemistry*; Cornell University Press: Ithaca, New York, 1953.
(19) Duyndam, A.; Odijk, T. *Langmuir* **1996**, *12*, 4718.
(20) Kramers, W. *J. Chem. Phys.* **1946**, *14*, 415.
(21) Bloomfield, V. A.; Zimm, B. H. *J. Chem. Phys.* **1966**, *44*, 315.
(22) Fukatsu, M.; Kurata, M. *J. Chem. Phys.* **1966**, *44*, 4539.
(23) Garcia Bernal, J. M.; Tirado, M. M.; Freire, J. J.; Garcia de la Torre, J. *Macromolecules* **1990**, *23*, 3357.
(24) Bond, A. M. *Modern polarographic methods in analytical chemistry*; Marcel Dekker: New York, 1980.
(25) Bard, A. J.; Faulkner, L. R. *Electrochemical methods. Fundamentals and Applications*; John Wiley: New York, 2001.
(26) Van Leeuwen, H. P.; Cleven, R. F. M. J.; Buffle, J. *Pure Appl. Chem.* **1989**, *61*, 255.
(27) Crow, D. R. *Polarography of metal complexes*; Academic Press: London, 1969.
(28) De Jong, H. G.; Van Leeuwen, H. P. *J. Electroanal. Chem.* **1987**, *235*, 1.
(29) Mota, A. M.; Correia dos Santos, M. M. In *Metal Speciation and Bioavailability in Aquatic Systems*; Tessier, A., Turner, D. R., Eds.; John Wiley: Chichester, U.K., 1995.
(30) De Jong, H. G.; Van Leeuwen, H. P. *J. Electroanal. Chem.* **1987**, *234*, 17.
(31) De Jong, H. G.; Van Leeuwen, H. P.; Holub, K. *J. Electroanal. Chem.* **1987**, *234*, 1.
(32) Cleven, R. F. M. J.; De Jong, H. G.; Van Leeuwen, H. P. *J. Electroanal. Chem.* **1986**, *202*, 57.
(33) Puy, J.; Cecilia, J.; Galceran, J.; Town, R. M.; Van Leeuwen, H. P. *J. Electroanal. Chem.*, submitted.
(34) Van Leeuwen, H. P. *Sci. Total Environ.* **1987**, *60*, 45.
(35) Garces, J. L.; Mas, F.; Cecila, J.; Puy, J.; Galceran, J.; Salvador, J. *J. Electroanal. Chem.* **2000**, *484*, 107.
(36) Schmatloch, S. Personal communication.
(37) Van Leeuwen, H. P.; Buffle, J.; Lovric, M. *Pure Appl. Chem.* **1992**, *64*, 1015.
(38) Flory, P. J. *Statistical Mechanics of Chain Molecules*; Hanser: Munich, 1989.
(39) Kienberger, F.; Patushenko, V. P.; Kada, G.; Gruber, H. J.; Riener, C.; Schindler, H.; Hinterdorfer, P. *Single Mol.* **2000**, *1*, 123.
(40) Puy, J.; Torrent, M.; Monne, J.; Cecila, J.; Galceran, J.; Salvador, J.; Garces, J. L.; Mas, F.; Berbel, J. *J. Electroanal. Chem.* **1999**, *457*, 229.
(41) Eigen, M. *Pure Appl. Chem.* **1963**, *6*, 97.
(42) Morel, F. M. M.; Hering, J. G. *Principles and Applications of Aquatic Chemistry*; John Wiley: New York, 1993.
(43) Lide, D. R., Ed.; *Handbook of Chemistry and Physics*; CRC Press: Boca Raton, FL, 2002.
(44) Van der Gucht, J.; Besseling, N. A. M.; Knoben, W.; Bouteiller, L.; Cohen Stuart, M. A. *Phys. Rev. E* **2003**, *67*, 051106.
(45) Langevin, D.; Rondelez, F. *Polymer* **1978**, *19*, 875.